

An optimized distributed fiber Bragg grating sensing system based on optical frequency domain reflectometry

Yuewen HAN (✉), Cheng CHENG

Optical Fiber Sensing Technology Research Center, Wuhan University of Technology, Wuhan 430070, China

© Higher Education Press and Springer-Verlag Berlin Heidelberg 2012

Abstract In this paper, the waveforms in time domain and frequency domain of two kinds of optical frequency domain reflectometry (OFDR) sensing systems are compared, which use common fiber Bragg grating (FBG) and chirped grating, respectively. The results show that chirped fiber grating with about 3 nm of full width at half maximum (FWHM) is helpful to reduce frequency noise evidently and makes the characteristic frequency distinct. OFDR distributed sensing system with chirped grating also offers longer available time, which makes it convenient to measure slow time-varying signal. Such OFDR distributed sensing system is supposed to be more suitable to be applied in bridge health monitoring, and it will improve the accuracy and reliability of the measurement.

Keywords fiber Bragg grating (FBG) sensor, optical frequency domain reflectometry (OFDR), strain, chirped grating

1 Introduction

Optical frequency domain reflectometry (OFDR) as one of key techniques in distributed sensing systems has been developed in recent years. It has been used for locating in surfaces diagnosing, such as gauge and cryogenic tanks, which are used in aerospace industry [1–4]. This paper focuses on the field of bridge health monitoring, where there are not so much application of this technique, and it leads to some improvement in the technical scheme.

Although measurement based on this technique sometimes seems slow, which takes about several seconds or more, OFDR technique still performed excellently, due to its some advantages, such as high resolution, reliability, simpleness, low cost, etc.

The highest resolution of OFDR technique is reported to

be 10 μm , and attracts much interest. In some situation, such high spatial resolution completely satisfies practical need, such as measurements of strain and temperature.

In temperature measurement, the lowest testable temperature is reported to be about 10 K [3], and there has been several techniques developed for intrinsic temperature compensation or testing both temperature and strain simultaneously [5–8].

Different forms of OFDR sensing system have been applied in engineering fields to test diverse parameters [1–4,9–11], the working wavelength bands reported are 850, 1300 and 1550 nm, but changing working wavelength does not help to increase the measurement accuracy.

Simulation based on coupled-mode theory and transfer matrices theory are also developed, and method of locating or calibration based on Fourier transfer is also studied [4,12], which help to improve the performance of this kind of sensing system.

Because common fiber Bragg grating (FBG) has very narrow full width at half maximum (FWHM) of its reflective spectrum, available time of the OFDR sensing system is very short, so it will not favor measurement for slow varying signal, or real-time observation. In this paper, an optimized OFDR sensing system is presented to overcome the above shortcomings, and the simulation of chirped grating reflective spectrum is also given.

2 Methods and results

2.1 Composition of OFDR system

Figure 1 shows the experimental setup of OFDR sensing system. The central wavelength of the tunable laser is 1310 nm, and the maximum span is 100 nm. The light output is injected into 1-by-2 coupler C1, and then part of light enters C2, a 2-by-2 coupler, others enter C3. Light is reflected by R1 and R2 and interferes with each other when they arrive at C1. The interfered signal is received by PD1,

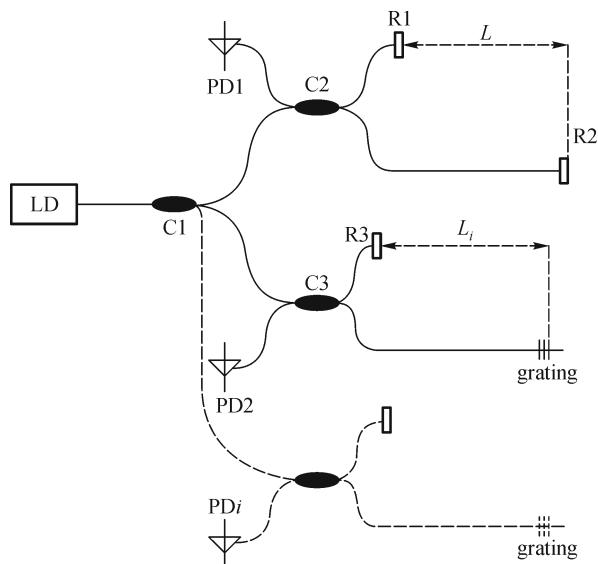


Fig. 1 Experimental setup of sensing system based on OFDR

and converted to voltage signal. In the branch of C3, the whole processing is as same as that in C2, except that one of reflector is substituted by a FBG or a series of FBGs. Signal from branch C3 or interferometer C3 is detected by PD2, which receives lights originally reflected from R3 and grating sequence. Due to the optical property of FBG, only light of very narrow bandwidth of the light source is reflected.

If the power of the light source is high enough, more branch pairs can be added to extend the system scale.

Since R1 and R3 in branches C2 and C3 are identical, they can be substituted by one mirror [10], i.e., sharing one mirror together. In fact, saving a branch means saving light power injected into measuring branches.

2.2 Measurement principle of OFDR

In branch C2, or called as arm 1, light reflected from R1 and R2 has a constant optical path difference of $2nL$, n is the effective index of the core of the fiber, L is the optical path difference (OPD) of two paths to the interferometer C2. Because lights from R1 and R2 have the same state of polarization, frequency, and constant optical path difference (the same phase difference), they can interfere with each other in C2, so the signal D1 detected by PD1 can be described as

$$D1 = \cos(2knL), \quad (1)$$

where n is the refractive index, L is the optical path difference of R1 and R2, k is the wave number of the light, defined by

$$k = 2\pi/\lambda, \quad (2)$$

where λ is wavelength of the light. The OFDR signals are

driven by wavelength tuning of the LD, it means that λ and k is time-varying parameter, so signal D1 is also time-varying curve, and the frequency of D1 is proportional to k , when other parameters are fixed. When the wavelength of the tunable laser, $\lambda(k)$, scans, from an initial set-up wavelength gradually and uniformly, D1 will act like a cosine curve with constant frequency, and it can be used to trigger sampling of PD2.

For the arm C3, each grating of FBG series on the optical fiber will reflect part of light injected in. But each one can be described by equation as D2, and its form is as same as Eq. (1). If strain or temperature change is added on one of the FBGs, its central wavelength will shift, so the shift of k of its own equation will result in change of the frequency of signal D2 (of PD2), the change value of frequency indicates the strain change on it [1,2,9]. So measurement is accomplished.

Because each FBG of the FBG series has different L_i , distance to R3, D2 will act as combination of many “D1” with different frequency. Then signal D2 can be described as

$$D2 = \sum_i R_i \cos(2knL_i), \quad (3)$$

R_i is reflective ratio of grating i and L_i is length difference of the corresponding grating i to R3.

Each frequency included in D2 represents a specific grating on the fiber. Gratings of different location correspond different frequency, so they can be distinguished and located.

Ideally if the FBGs in a series are located continuously, each point in the FBG can be measured, and the system is a distributed sensing system; if the FBGs are lined up with a small interval, the system can be used as a quasi-distributed sensing system.

2.3 Schemes with common gratings

Wavelengths of 1310 and 1550 nm are both feasible except tiny ignorable difference in OFDR sensing system. In this experiment, 1310 nm tunable laser is adopted.

First, common FBGs are used to be sensor body, whose central wavelength is about 1298.4 nm and the FWHM is about 0.07 nm, shown in Fig. 2. So the central wavelength of the FBGs is consistent to the light source.

As mentioned above, this FBG, R3 and C3 together compose an interferer, time varying wavelength of laser results in time varying D2 signal, which is shown in Fig. 3. Figure 4 is frequency spectrum of D2. In Fig. 3, the received signal is input at AC coupling mode and the limitation of frequency width is off.

Figure 4 shows a characteristic frequency of signal D2, during observation. It can be easily deduced from Eq. (3) that D1 should have several simple conspicuous frequencies: one is zero frequency (direct current); another is

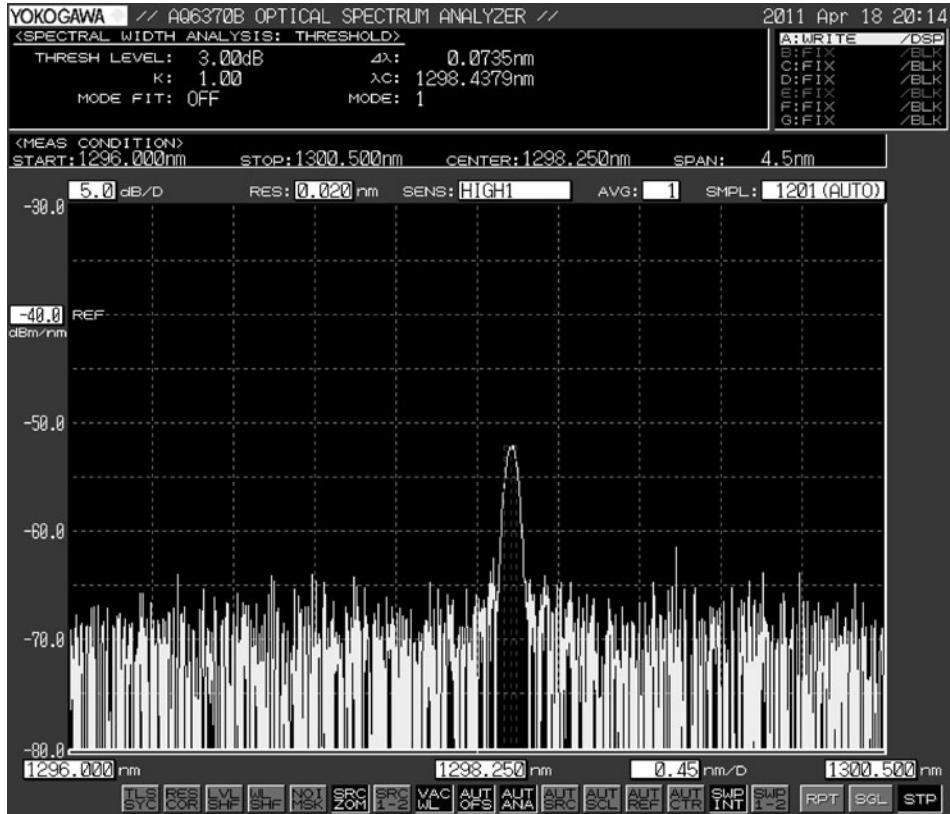


Fig. 2 Reflectivity spectrum of common FBG in this experiment

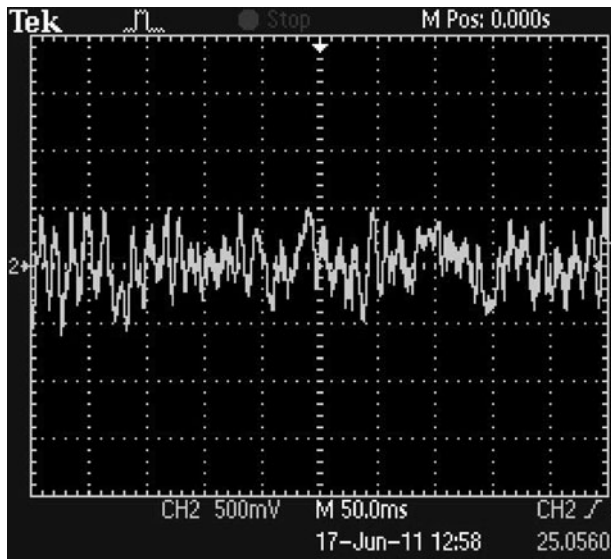


Fig. 3 D2 signal using common grating at 1298 nm

correspondent to the specific FBG. While Fig. 4 shows a spectrum including much frequency elements irrelevant, which will disturb the justice to the sensing physical quantity measured and lower its accuracy. Beside main frequencies of D2 signal, other frequency irrelevant should

be regarded as noise. In Fig. 4, it can be found that there is more noise than that of our expectation, which will not satisfy subsequent signal processing device. Figure 4 is acquired at about 1298 nm, and the results at other wavelengths are similar to those shown in Fig. 4, so the difference between them may be resulted from system error.

As the performance of other components has very high stability, suitable gratings should be taken into account to reduce such system error. Only the FBGs are manufactured by our own in this system, so better FBG or other type of grating should be tried to use to reduce such system error.

The main quality parameters of FBG are in its reflective spectrum, including available reflective bandwidth and maximum peak value.

Under the scanning speed of 1 nm/s, the wave-band of 0.07 nm will be merely covered within 0.07 s. Besides, FBG spectrum is usually regarded as Gaussian curve, so, time-varying reflect ratio must result in the fluctuation of D2 signal, though laser power is constant during the whole scanning. That means the D2 signal will be more stable if grating reflective spectrum has a flat and wider crest.

The broadband mirror and the chirped grating have same reflection property, but the latter is more useful because the sensitivity is also demanded to certain degree, which is relative to its reflective height. The height of its reflective spectrum is flexible to be manufactured.

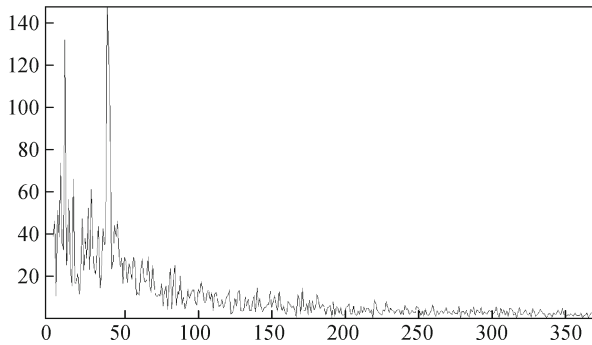


Fig. 4 Frequency spectrum of D2 signal

2.4 Schemes based on chirped gratings

To predict the optical property of the chirped grating, some simulation and calculation are given below. For a typical non-uniform waveguide, coupled-mode theory and transfer matrices theory are suitable. The software OptiGrating 4.2 is adopted in this simulation to simplify the calculation based on those theories. The simulation result is given in Fig. 5.

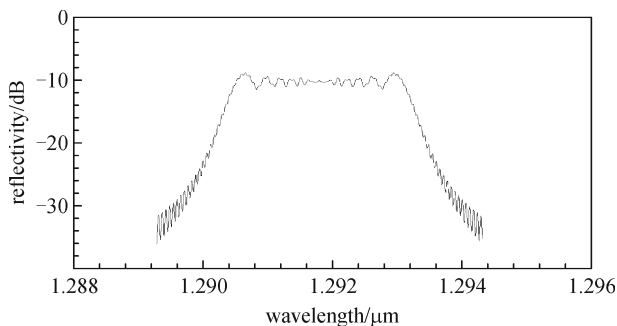


Fig. 5 Simulation of chirped grating reflective spectrum

In the simulation, a 1 cm-long chirped grating is assumed, and its central wavelength of about 1297 nm is set to resemble the grating mask, which is shown in Fig. 5. The refractive index of optical fiber core is set to be 1.4600, the periods of chirp step is set to be linear, the grating profile is set to a sine function, and the total chirp is about 1.0395.

According to the parameters of simulation above, a real chirped grating whose central wavelength of 1291.8 nm is manufactured by our own, whose FWHM is 3.03 nm. Its reflective spectrum is shown in Fig. 6. Thus, scanning time covering the flat crest is up to 3.03 s, which is rather stable for subsequent device to processing.

Figure 7 shows the waveform acquired by PD2 using chirped grating sensor whose central wavelength is 1291 nm, and Fig. 8 shows its frequency spectrum, from which the location of chirped grating and strain rested on can be determined. The situation of signal in Fig. 7 is the

same as that in Fig. 3.

As compared between Figs. 4 and 8, it is clearly found that D2 signal of OFDR sensing system using chirped grating sensor is much better than that using common FBG sensor, because noise frequency is reduced more after chirped grating is used, and main frequency of the specific grating is more distinct for calculation. So accuracy and reliability increase under the same situation.

2.5 Analysis for the optimized system

The performance of D2 signal after chirped grating adopted can be expressed as follow. Because the chirped grating is a wideband reflector for the laser, its profile of reflective spectrum is a rectangle function, especially when the crest of spectrum is controlled well to be strictly flat.

$$D2 = \sum_i R_i \text{rect}(\lambda) \cos(2knL_i), \quad (4)$$

where $\text{rect}(\lambda)$ is the function of chirped grating reflective spectrum, λ is variable wavelength scanning in the designed spectrum. In this simulation, λ of the chirped grating is varying from 1290.2985 to 1293.3015 nm.

If only one chirped grating is used in a fiber, the equation of signal D2 should be changed into:

$$D2 = \text{rect}(\lambda) \cos(2knL). \quad (5)$$

Regarding the crest of chirped grating reflective spectrum is usually not absolute flat; the rectangle function in Eq. (5) can also be substituted as its Fourier decomposing form, including limited items. The latter form of the equation maybe cause smaller error for a real chirped grating reflective spectrum.

But the crest fluctuation of the chirped grating reflective spectrum is comparatively slow for the scanning speed of the tunable laser in this system, and the step of wavelength scanning can be even set to be 1 pm. So during the processing, the reflect ratio of chirped grating is stable and the fluctuation will not disturb the measurement.

3 Discussion

The noise component of the data are reduced evidently due to the chirped grating in OFDR system, so the signal noise ratio (SNR) of the whole measurement increases, which means that gratings of lower reflective ratio can be used, and then more gratings can be written in an optical fiber. So chirped grating will favor OFDR system of larger scale.

Chirped grating offers continuous and uniform reflective spectrum during the whole scanning process, but the common FBG offers sharp reflective peak. That means the output signal will not fluctuate abruptly when the laser scans, if the power of the light source is very stable. So system error resulting from signal power fluctuation is

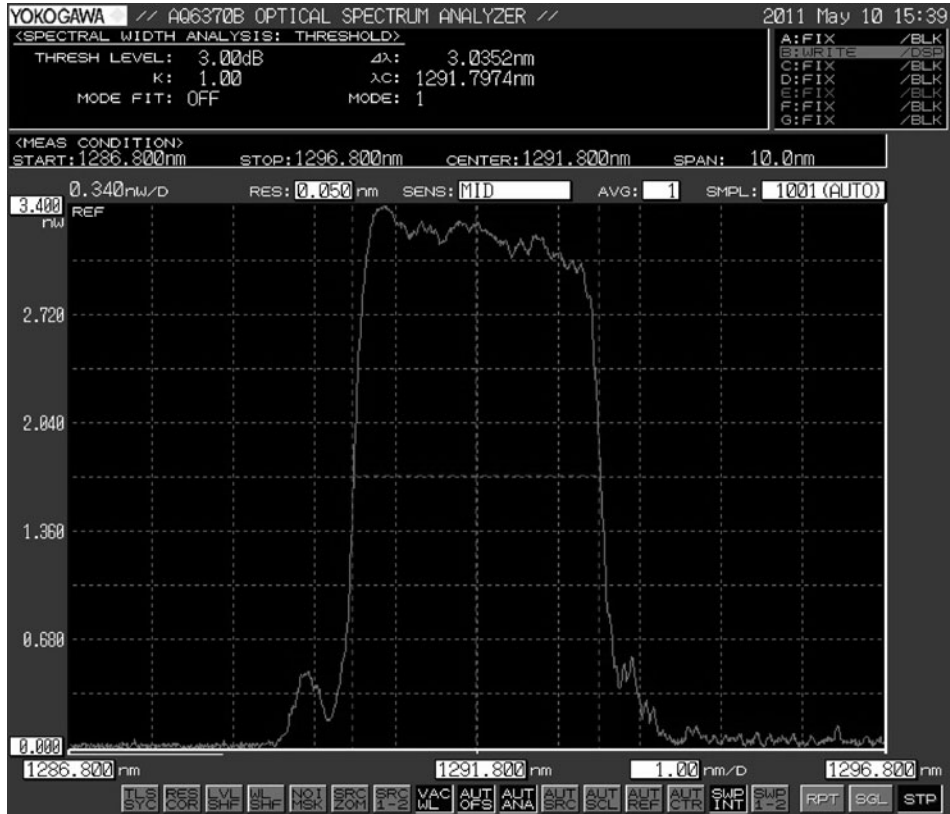


Fig. 6 Chirped grating spectrum in this experiment

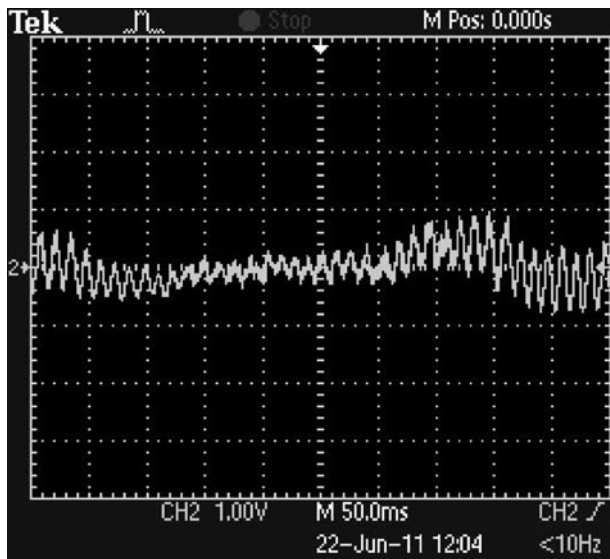


Fig. 7 D2 signal using chirped grating at 1291 nm

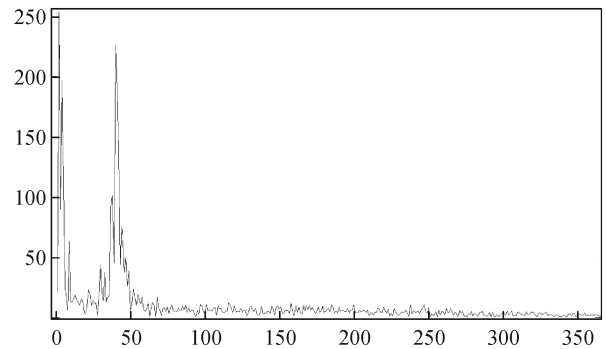


Fig. 8 Frequency spectrum of D2 signal

reduced and better accuracy will be acquired consequently.

Stable effective output signal of longer time is offered due to broader bandwidth of chirped grating in OFDR system, also. The effective scanning time is about 3 s, which meets our requirements, and it is even enough for observation. The most important is that strain/temperature

change or other variable of slow time-varying can also be recorded during their whole changing process, if the changing time it cost is smaller than the scanning time. For example, the typical vibration frequency of a huge bridge is usually within 1 Hz, or even smaller, which means sampling time of more than 1 s is necessary.

Performance of optimized OFDR using chirped grating is better than that of common FBG, although their measurement principle and the sensing system is similar. Such optimized distributed sensing system of OFDR is hopeful for further application in huge construct health monitoring.

Acknowledgements This work was supported by the Fundamental Research Funds for the Central Universities (No. WHUT 2011-IV-002).

References

1. Childers B A, Froggatt M E, Allison S G, Moore T C, Hare D A, Batten C F, Jegley D C. Use of 3000 Bragg grating strain sensors distributed on four eight-meter optical fibers during static load tests of a composite structure. *Proceedings of the Society for Photo-Instrumentation Engineers*, 2001, 4332: 133–142
2. Jegley D C, Bush H G. Structural Testing of a Stitched/Resin Film Infused Graphite-Epoxy Wing Box. NASA LaRC Technical Memorandum, 2001
3. Wu M C, Prosser W H. Simultaneous temperature and strain sensing for cryogenic applications using dual-wavelength fiber Bragg gratings. *Proceedings of the Society for Photo-Instrumentation Engineers*, 2003, 5191(1): 208–213
4. Igawa H, Ohta K, Kasai T, Yamaguchi I, Murayama H, Kageyama K. Distributed measurements with a long gauge FBG sensor using optical frequency domain reflectometry. *Journal of Solid Mechanics and Materials Engineering*, 2008, 2(9): 1242–1252
5. Xu M G, Archambault J L, Reekie L, Dakin J P. Discrimination between strain and temperature effects using dual-wavelength fiber grating sensors. *Electronics Letters*, 1994, 30(13): 1085–1087
6. Patrick H J, Williams G M, Kersey A D, Pedrazzani J R, Vengsarkar A M. Hybrid fiber Bragg grating/long period fiber grating sensor for strain/temperature discrimination. *IEEE Photonics Technology Letters*, 1996, 8(9): 1223–1225
7. Kanellopoulos S E, Handerek V A, Rogers A J. Simultaneous strain and temperature sensing with photogenerated in-fiber gratings. *Optics Letters*, 1995, 20(3): 333–335
8. Brady G P, Kalli K, Webb D J, Jackson D A, Reekie L, Archambault J L. Simultaneous measurement of strain and temperature using the first- and second-order diffraction wavelengths of Bragg gratings. *IEE Proceedings of Optoelectronics*, 1997, 144(3): 156–161
9. Kersey A D, Davis M A, Patrick H J, LeBlanc M, Koo K P, Askins C G, Putnam M A, Friebele E J. Fiber grating sensors. *Journal of Lightwave Technology*, 1997, 15(8): 1442–1463
10. Froggatt M, Moore J. Distributed measurement of static strain in an optical fiber with multiple Bragg gratings at nominally equal wavelengths. *Applied Optics*, 1998, 37(10): 1741–1746
11. Froggatt M. Distributed measurement of the complex modulation of a photoinduced Bragg grating in an optical fiber. *Applied Optics*, 1996, 35(25): 5162–5164
12. Abdi A M, Suzuki S, Schülzgen A, Kost A R. Fiber bragg grating array calibration. *Proceedings of the Society for Photo-Instrumentation Engineers*, 2005, 5765: 552–563